

Reproduction of Forward and Backward Propagations on Dendrites by Multi-compartment Asynchronous Cell Automaton Neuron

Naoki Shimada and Hiroyuki Torikai

Abstract—The neuron is roughly divided into three parts: soma, dendrite, and an axon. In this paper, a multi-compartment neuron model the dynamics of which is described by an asynchronous cellular automaton is presented. It is shown that the model can reproduce typical propagations of action potentials from dendrites to a soma (forward propagation) and from a soma to dendrites (backward propagation).

I. INTRODUCTION

Many neuron models have been proposed so far [1]–[2]. Among them, Hodgkin-Huxley-type conductance based models and Izhikevich-type simplified models are typical ones. Like these models, many neuron models have continuous states and a continuous time and thus they are described by ordinary differential equations (ab. ODEs). On the other hand, recently, several types of asynchronous cellular automaton neuron models have been proposed [3] [4]. The asynchronous cellular automaton neuron model has discrete states and a continuous (state transition) time, and thus it belongs to a different class of dynamical system from the traditional ODE neuron models. The advantages of the asynchronous cellular automaton neuron model include low hardware cost and dynamically reconfigurable capability [3] [4].

The neuron is roughly divided into three parts: soma, dendrites, and an axon. It has been pointed out that the physical structure of the dendrite (which is sometimes very complicated like Purkinje cell) plays certain roles in information processing of neurons [5]–[7]. A variety of phenomena can be observed in the dendrite, e.g., propagations and failures of propagations of action potentials from dendrites to a soma (i.e., forward propagations and their failures) and propagations and failures of propagations of action potentials from a soma to dendrites (i.e., backward propagations and their failures). In order to analyze such dendritic phenomena, multi-compartment methods have been utilized [8]–[11].

In this paper, a multi-compartment neuron model based on the asynchronous cellular automaton is presented. It is shown that the model can reproduce typical forward and backward propagations of action potentials and their failures. It is also shown that the model can be implemented by a smaller number of transistors compared to

Naoki Shimada is with the Department of Systems Innovation, Graduate School of Engineering Science, Osaka University, 1-3, Machikaneyama-cho, Toyonaka, Osaka 560-8531, Japan

Hiroyuki Torikai is with the Department of Computer Science, Faculty of Computer Science and Engineering, Kyoto Sangyo University, Motoyama, Kamigamo, Kita-Ku, Kyoto-City 603-8555, Japan

This work was supported by the support center for advanced telecommunications technology research (SCAT) and KAKENHI Grant Number 24700225.

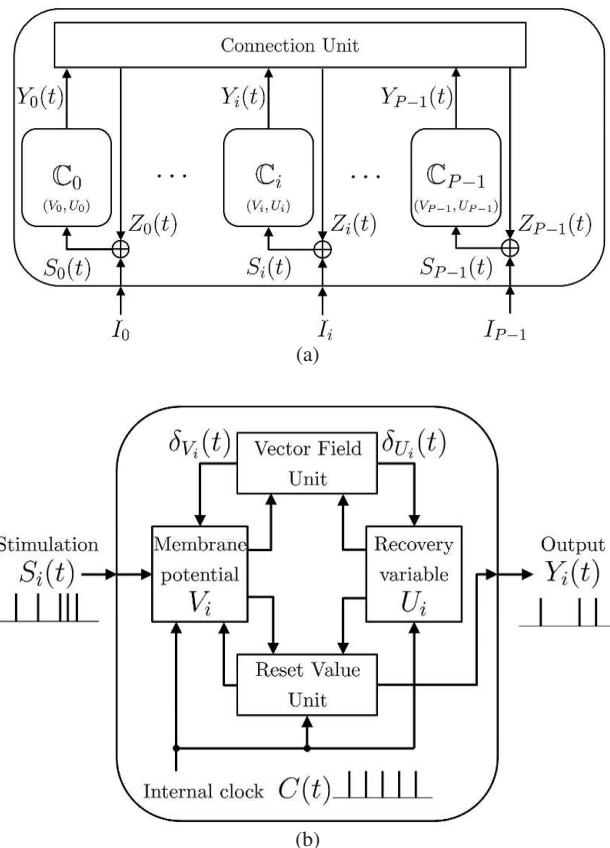


Fig. 1. (a) Whole structure of a multi-compartment neuron model. \oplus represents the arithmetic sum. (b) Single compartment based on our previous soma's membrane model [3].

conventional multi-compartment neuron models. This paper includes highly generalized analysis results and novel experimental results compared to our short conference manuscript [12] in which very preliminary and limited results on the model have been discussed.

II. MULTI-COMPARTMENT NEURON MODEL AND REPRODUCTIONS OF DENDRITIC ACTION POTENTIAL PROPAGATIONS

In this section a multi-compartment neuron model, the nonlinear dynamics of which is described by an asynchronous cellular automaton, is presented. Fig. 1(a) shows a sketch of the whole structure of the multi-compartment neuron model, where each compartment is indexed by $i \in \{0, 1, \dots, P-1\}$, the i -th compartment is denoted by C_i , and P is the number of the compartments. As shown in Fig. 1(b), each compartment C_i accepts a common internal

clock $C(t)$, where $t \in [0, \infty)$ is a continuous-time. In this paper, the following internal clock $C(t)$ with a normalized period 1 is focused on.

$$C(t) = \begin{cases} 1 & \text{if } t = 0, 1, 2, \dots, \\ 0 & \text{otherwise.} \end{cases}$$

Also, each compartment \mathbb{C}_i can accept the following stimulation $S_i(t)$.

$$S_i(t) = \begin{cases} s_n^i \in \{1, 2, 3, \dots\} & \text{if } t = t_n^i \in \mathbb{R}^+, \\ 0 & \text{otherwise,} \end{cases}$$

where t_n^i is the n -th spike position of the stimulation $S_i(t)$.

A. Dynamics of single compartment

In this subsection, a single compartment is presented based on our previous soma's membrane model [3]. As shown in Fig. 1(b), the single compartment \mathbb{C}_i consists of the following two registers and two memoryless units, where “ \equiv ” represents the “definition” hereafter.

- 1) A membrane register having an integer state

$$V_i \in \mathbf{N}_i \equiv \{0, 1, \dots, N_i - 1\}$$

corresponding to a membrane potential of the compartment \mathbb{C}_i . V_i is referred to as a *membrane potential*.

- 2) A recovery register having an integer state

$$U_i \in \mathbf{M}_i \equiv \{0, 1, \dots, M_i - 1\}$$

corresponding to a channel dynamics of the compartment \mathbb{C}_i . U_i is referred to as a *recovery variable*.

- 3) A memoryless *vector field unit* consisting of logic gates and reconfigurable wires, which determines a sub-threshold vector field of the compartment \mathbb{C}_i .
- 4) A memoryless *reset value unit* consisting of logic gates and reconfigurable wires, which is used to realize a super-threshold firing reset of the compartment \mathbb{C}_i .

As shown in Fig. 1(b), the vector field unit accepts the membrane potential $V_i \in \mathbf{N}_i$ and the recovery variable $U_i \in \mathbf{M}_i$. Also, the vector field unit outputs signals $\delta_{V_i} \in \{-1, 0, 1\}$ and $\delta_{U_i} \in \{-1, 0, 1\}$. Hence the vector field unit works as the following functions D_{V_i} and D_{U_i} .

$$\begin{aligned} \delta_{V_i} &= D_{V_i}(V_i, U_i), \quad D_{V_i} : \mathbf{N}_i \times \mathbf{M}_i \rightarrow \{-1, 0, 1\}, \\ \delta_{U_i} &= D_{U_i}(V_i, U_i), \quad D_{U_i} : \mathbf{N}_i \times \mathbf{M}_i \rightarrow \{-1, 0, 1\}. \end{aligned}$$

In order to realize proper neuron-like behaviors of the multi-compartment neuron model, in this paper the following design procedure of the vector field unit is used. First, the entire phase plane $\mathbf{N}_i \times \mathbf{M}_i$ is divided into the following five disjoint subspaces $\{\mathbf{S}_i^{++}, \mathbf{S}_i^{+-}, \mathbf{S}_i^{-+}, \mathbf{S}_i^{--}, \mathbf{S}_i^0\}$.

$$\begin{aligned} \mathbf{S}_i^{++} &\equiv \{(V_i, U_i) \mid U_i < f_{V_i}(V_i), U_i \leq f_{U_i}(V_i)\}, \\ \mathbf{S}_i^{+-} &\equiv \{(V_i, U_i) \mid U_i \geq f_{V_i}(V_i), U_i < f_{U_i}(V_i)\}, \\ \mathbf{S}_i^{-+} &\equiv \{(V_i, U_i) \mid U_i \leq f_{V_i}(V_i), U_i > f_{U_i}(V_i)\}, \\ \mathbf{S}_i^{--} &\equiv \{(V_i, U_i) \mid U_i > f_{V_i}(V_i), U_i \geq f_{U_i}(V_i)\}, \\ \mathbf{S}_i^0 &\equiv \{(V_i, U_i) \mid (V_i, U_i) \notin \mathbf{S}_i^{++} \cup \mathbf{S}_i^{+-} \cup \mathbf{S}_i^{-+} \cup \mathbf{S}_i^{--}\}, \end{aligned}$$

where the functions $f_{V_i} : \mathbf{N}_i \rightarrow \{-1, 0, \dots, M_i\}$ and $f_{U_i} : \mathbf{N}_i \rightarrow \{-1, 0, \dots, M_i\}$ work as borders of the subspaces $\{\mathbf{S}_i^{++}, \mathbf{S}_i^{+-}, \mathbf{S}_i^{-+}, \mathbf{S}_i^{--}, \mathbf{S}_i^0\}$ and are defined by

$$\begin{aligned} f_{V_i}(V_i) &= \alpha_i(\lfloor k_{i1}V_i^2 + k_{i2}V_i + k_{i3} \rfloor), \\ f_{U_i}(V_i) &= \alpha_i(\lfloor k_{i4}V_i + k_{i5} \rfloor), \\ k_{i1} &= \frac{f_{i1}M_i}{N_i^2}, \quad k_{i2} = -2k_{i1} \lfloor f_{i2}N_i \rfloor, \\ k_{i3} &= k_{i1}(\lfloor f_{i2}N_i \rfloor)^2 + \lfloor f_{i3}M_i \rfloor, \\ k_{i4} &= \frac{f_{i4}M_i}{N_i}, \quad k_{i5} = \lfloor f_{i5}M_i \rfloor, \\ \alpha_i(x) &= \begin{cases} -1 & \text{if } x < -1, \\ x & \text{if } -1 \leq x \leq M_i, \\ M_i & \text{otherwise,} \end{cases} \end{aligned}$$

where “ $\lfloor \cdot \rfloor$ ” is the floor function. Typical examples of the border functions ($f_{V_i}(V_i), f_{U_i}(V_i)$) and resulting subspaces $\{\mathbf{S}_i^{++}, \mathbf{S}_i^{+-}, \mathbf{S}_i^{-+}, \mathbf{S}_i^{--}, \mathbf{S}_i^0\}$ are shown in Fig. 2. Second, using the subspaces $\{\mathbf{S}_i^{++}, \mathbf{S}_i^{+-}, \mathbf{S}_i^{-+}, \mathbf{S}_i^{--}, \mathbf{S}_i^0\}$, the vector field unit is designed to be a state-dependent one as follows.

$$\begin{aligned} \delta_{V_i} &= D_{V_i}(V_i, U_i) \\ &= \begin{cases} 1 & \text{if } (V_i, U_i) \in \mathbf{S}_i^{++} \cup \mathbf{S}_i^{+-}, V_i \neq N_i - 1, \\ -1 & \text{if } (V_i, U_i) \in \mathbf{S}_i^{-+} \cup \mathbf{S}_i^{--}, V_i \neq 0, \\ 0 & \text{if } (V_i, U_i) \in \mathbf{S}_i^0, \end{cases} \end{aligned}$$

$$\begin{aligned} \delta_{U_i} &= D_{U_i}(V_i, U_i) \\ &= \begin{cases} 1 & \text{if } (V_i, U_i) \in \mathbf{S}_i^{++} \cup \mathbf{S}_i^{-+}, U_i \neq M_i - 1, \\ -1 & \text{if } (V_i, U_i) \in \mathbf{S}_i^{+-} \cup \mathbf{S}_i^{--}, U_i \neq 0, \\ 0 & \text{if } (V_i, U_i) \in \mathbf{S}_i^0. \end{cases} \end{aligned}$$

The resulting vector field unit is characterized by the parameters $(M_i, N_i, f_{i1}, f_{i2}, f_{i3}, f_{i4}, f_{i5})$. The vector field unit determines the sub-threshold vector field of the compartment \mathbb{C}_i as follows. Let us introduce the following subset \mathbf{L}_i of the entire phase plane $\mathbf{N}_i \times \mathbf{M}_i$.

$$\mathbf{L}_i \equiv \{(V_i, U_i) \mid V_i = N_i - 1, U_i \in \mathbf{M}_i\} \subset \mathbf{N}_i \times \mathbf{M}_i,$$

where a point on \mathbf{L}_i is represented by its U_i -coordinate. The subset \mathbf{L}_i corresponds to a firing threshold (or spike cutoff level) of a spiking neuron model and thus is referred to as a *firing threshold*. Now assume the state vector (V_i, U_i) is *not* in the firing threshold \mathbf{L}_i . In this case, the vector field unit determines transitions of the state vector (V_i, U_i) as follows.

Sub-threshold dynamics induced by internal clock:

$$\begin{cases} V_i := V_i + \delta_{V_i}, \\ U_i := U_i + \delta_{U_i}, \end{cases} \quad \text{if } (V_i, U_i) \notin \mathbf{L}_i \text{ and } C(t) = 1, \quad (1)$$

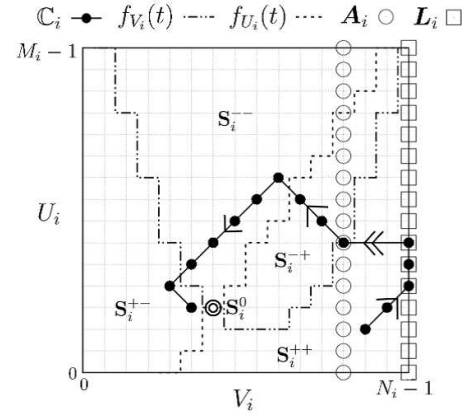
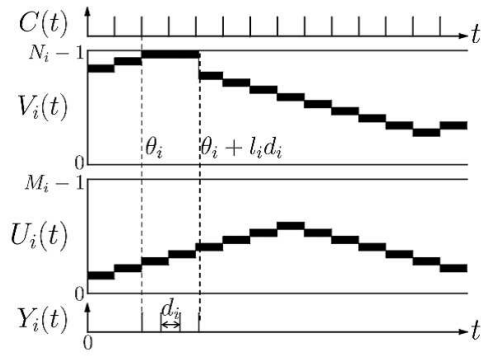
where “ $:=$ ” represents the “instantaneous transition” hereafter. Fig. 2(a) shows an example of the autonomous sub-threshold dynamics of the compartment \mathbb{C}_i .

As shown in Fig. 1(b), the reset value unit accepts the recovery variable $U_i \in \mathbf{M}_i$ and outputs a signal $A_i(U_i) \in \mathbf{N}_i$. Hence the reset value unit works as the following function A_i .

$$A_i : \mathbf{M}_i \rightarrow \mathbf{N}_i.$$

The function A_i is characterized by the parameters $(A_i(0), A_i(1), \dots, A_i(M_i - 1))$. In order to describe the

(a)



(b)

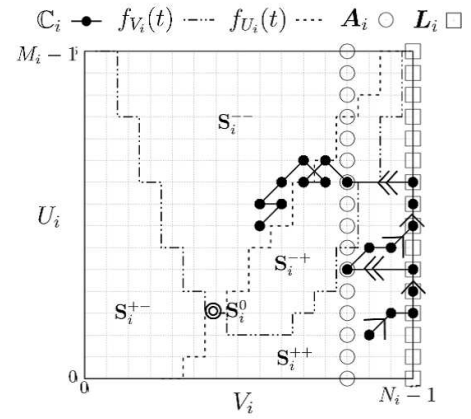
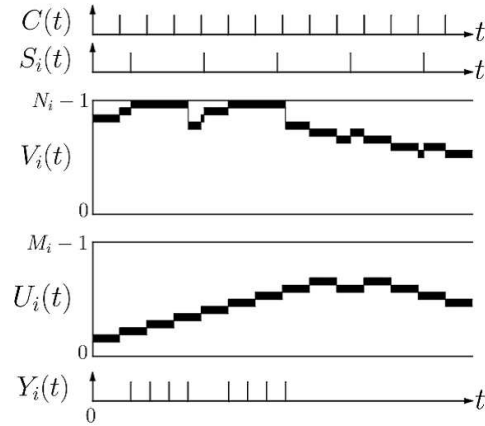


Fig. 2. Time waveforms (left) and phase plane trajectories (right) of the compartment \mathbb{C}_i .

$N_i = M_i = 16$, $\mathbf{f}_i = (4.5, 0.55, 0.15, 1.5, -0.35)$, $A_i(U_i) = 12$, $B_i = 4$, $d_i = 0.7$. (a) Autonomous single compartment. (b) Non-autonomous single compartment. $S_i = 1$ if $t = 1.4 + 2.7(n - 1)$ and $(n = 1, 2, 3, \dots)$, and $S_i(t) = 0$ otherwise.

super-threshold dynamics, let us introduce the following notation.

$\theta_i \equiv$ the moment when the state vector (V_i, U_i) reaches the firing threshold \mathbf{L}_i .

Now assume the state vector (V_i, U_i) reaches the firing threshold \mathbf{L}_i at $t = \theta_i$. In this case, the firing unit determines transitions of the state vector (V_i, U_i) as follows.

Super-threshold dynamics

$$\begin{cases} V_i := A_i(U_i) & \text{if } (V_i, U_i) \in \mathbf{L}_i \text{ and } t = \theta_i + l_i d_i, \\ U_i := U_i + \delta_{U_i} & \text{if } (V_i, U_i) \in \mathbf{L}_i \text{ and } C(t) = 1, \end{cases} \quad (2)$$

where $d_i > 0$ is a real parameter and $l_i > 0$ is an integer parameter. Fig. 2(a) shows an example of the super-threshold dynamics of the compartment \mathbb{C}_i . It can be seen that if the state vector (V_i, U_i) reaches the firing threshold \mathbf{L}_i at $t = \theta_i$, then it stays in the firing threshold \mathbf{L}_i for the time duration $\theta_i \leq t \leq \theta_i + l_i d_i$. During this stay, the compartment \mathbb{C}_i outputs the following spike-train Y_i .

Output spike-train

$$Y_i(t) = \begin{cases} 1 & \text{if } t = \theta_i, \theta_i + d_i, \dots, \theta_i + l_i d_i, \\ 0 & \text{otherwise.} \end{cases} \quad (3)$$

Fig. 2(a) shows an example of the output spike-train $Y_i(t)$ of the compartment \mathbb{C}_i .

As shown in Fig. 1(b), the membrane register accepts the stimulation $S_i(t)$. The stimulation $S_i(t)$ induces transitions of the state vector (V_i, U_i) as follows.

Stimulation induced sub-threshold dynamics:

$$V_i := V_i + S_i \quad \text{if } (V_i, U_i) \notin \mathbf{L}_i \text{ and } S_i(t) \neq 0. \quad (4)$$

Fig. 2(b) shows an example of the stimulation-induced sub-threshold dynamics of the compartment \mathbb{C}_i .

Remark 1 (asynchronous dynamics of single compartment) :

The state transition induced by the internal clock $C(t)$ in Equation (1) and the state transition induced by the stimulation $S_i(t)$ in Equation (4) can occur asynchronously. So, the single compartment has the discrete states (V_i, U_i) and the continuous transition time t . Hence, from a dynamical system viewpoint, the single compartment is an asynchronous cellular automaton.

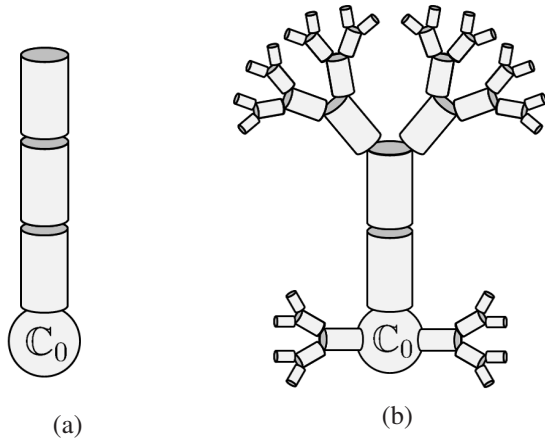


Fig. 3. Examples of multi-compartment neuron model. (a) $P = 4$ [8]. (b) $P = 47$ [9].

B. Multi-compartment neuron model

The compartments $\{C_0, \dots, C_{P-1}\}$ are connected via the output spike-trains $\{Y_0(t), \dots, Y_{P-1}(t)\}$ as follows.

Connections of compartments:

$$Z_i(t) = \sum_{j=0}^{P-1} w_{i,j} Y_j(t),$$

where $w_{i,j} \in \{0, 1\}$ is a parameter, which forms the following *connection matrix* \mathbf{W} .

$$\mathbf{W} = \begin{pmatrix} w_{0,0} & \cdots & w_{0,P-1} \\ \vdots & & \vdots \\ w_{P-1,0} & \cdots & w_{P-1,P-1} \end{pmatrix}$$

For example, the multi-compartment neuron model in Fig. 3(a) is characterized by the following connection matrix \mathbf{W} .

$$\mathbf{W} = \begin{pmatrix} 0 & 1 & 0 & 0 \\ 1 & 0 & 1 & 0 \\ 0 & 1 & 0 & 1 \\ 0 & 0 & 1 & 0 \end{pmatrix}$$

In addition to the spike-train $Z_i(t)$, each compartment C_i can accept (not necessarily) the following *external stimulation spike-train* $I_i(t)$.

$$I_i(t) = \begin{cases} 1 & \text{if } t \in \{q_1^i, q_2^i, \dots\}, \\ 0 & \text{otherwise,} \end{cases}$$

where q_n^i is the n -th spike position of the external stimulation spike-train $I_i(t)$. As shown in Fig. 1(a), each compartment C_i accepts the spike-train $Z_i(t)$ from the other compartments and the external stimulation spike-train $I_i(t)$ as follows.

Stimulation to compartment:

$$S_i(t) = Z_i(t) + I_i(t) = \sum_{j=0}^{P-1} w_{i,j} Y_j(t) + I_i(t). \quad (5)$$

As a result, the dynamics of the multi-compartment neuron model is described by Equations (1), (2), (3), (4), and (5).

Fig. 4 shows typical effects of the connection from the i -th compartment C_i to the j -th compartment C_j . In Fig. 4(a), the

compartment C_i has a short spike period $d_i = 0.35$, which corresponds to a strong connection to other compartments. In this case, the output spike-train $Y_i(t)$ of the compartment C_i leads to generation of the output spike-train $Y_j(t)$ of the compartment C_j . In Fig. 4(b), the compartment C_i has a long spike period $d_i = 0.7$, which corresponds to a weak connection to other compartments. In this case, the output spike-train $Y_i(t)$ of the compartment C_i weakly affects the behavior of the compartment C_j and the compartment C_j does not output a spike-train $Y_j(t)$. In Fig. 4(c), the compartment C_i has the same weak connection as the case of Fig. 4(b). In addition, both compartments accept low frequency external stimulation spike-trains $n_i(t)$ and $n_j(t)$, i.e.,

$$\begin{aligned} S_i(t) &= Z_i(t) + I_i(t) + n_i(t), \\ S_j(t) &= Z_j(t) + n_j(t). \end{aligned}$$

These external stimulation spike-trains $n_i(t)$ and $n_j(t)$ correspond to weak background noises around a neuron. In this case, the output spike-train $Y_i(t)$ of the compartment C_i leads to generation of the output spike-train $Y_j(t)$ of the compartment C_j .

Remark 2 (asynchronous dynamics of multi-compartment model) : As mentioned in Remark 1, the single compartment is an asynchronous cellular automaton. Hence the presented multi-compartment neuron model can be regarded as a network of asynchronous cellular automata, which is especially designed to reproduce dendritic phenomena.

C. Reproductions of dendritic phenomena

In this subsection, the multi-compartment neuron model in Fig. 5(a) is focused on, where its connection matrix is

$$\mathbf{W} = \begin{pmatrix} 0 & 1 & 0 & 0 & 0 \\ 1 & 0 & 1 & 0 & 0 \\ 0 & 1 & 0 & 1 & 1 \\ 0 & 0 & 1 & 0 & 0 \\ 0 & 0 & 1 & 0 & 0 \end{pmatrix}.$$

Let us introduce the following words for convenience of explanations.

Somatic compartment. For simplicity, the 0-th compartment C_0 is used as a somatic compartment (i.e., a cell body compartment) as shown in Fig. 5(a).

Terminal compartment. In Fig. 5(a), the compartment C_3 is connected to exactly one compartment C_2 . Such a compartment is referred to as a *terminal compartment*. In Fig. 5(a), the compartment C_4 is also a terminal compartment.

Relay compartment. In Fig. 5(a), the compartment C_1 is connected to more than one compartment. Such a compartment is referred to as a *relay compartment*. In Fig. 5(a), the compartment C_2 is also a relay compartment.

Action potential. If the compartment C_i outputs a spike, the corresponding wave of the membrane potential $V_i(t)$ is said to form an *action potential*. For example, the membrane potential $V_i(t)$ in Fig. 4(a) forms an action potential.

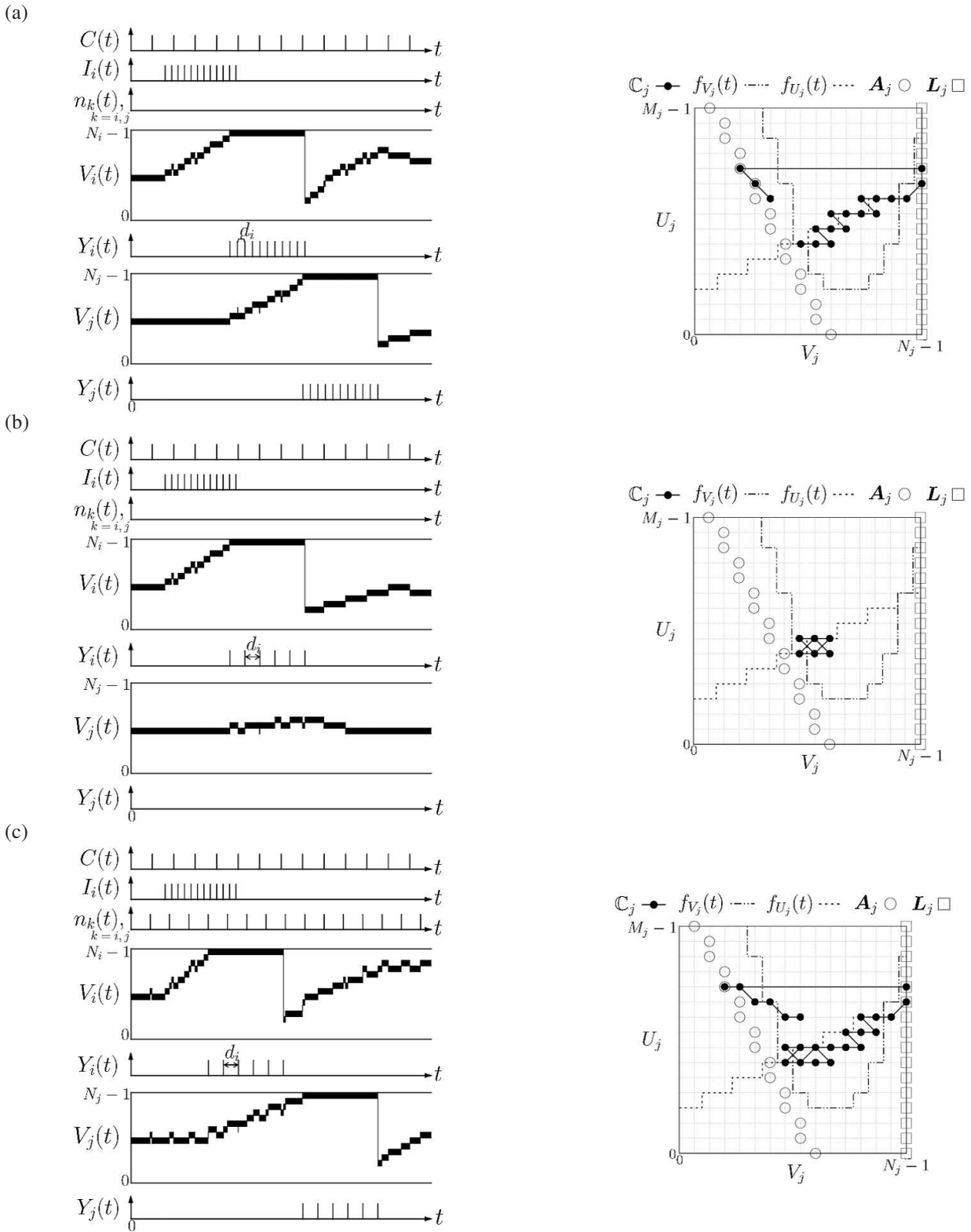


Fig. 4. Time waveforms (left) and phase plane trajectories (right) of the multi-compartment neuron model.

$P = 2$, $w_{0,0} = w_{1,1} = 0$, $w_{0,1} = w_{1,0} = 1$. $(M_k, N_k, f_{k1}, f_{k2}, f_{k3}, f_{k4}, f_{k5}) = (16, 16, 7.0, 0.65, 0.2, 0.5, 0.2)$, $A_k(U_k) = \lfloor -0.5U_k \rfloor + \lfloor 0.6N_k \rfloor$, $q_m^i = 1.6 + 0.3(m-1)$, $1.6 \leq q_m^i < 5$, and $m = 1, 2, 3, \dots$ for $k = i, j$. (a) Strong connection. $l_k = 10$, $d_k = 0.35$, and $l_k d_k = 3.5$ for $k = i, j$. (b) Weak connection. $l_k = 5$, $d_k = 0.7$, and $l_k d_k = 3.5$ for $k = i, j$. (c) Weak connection plus weak background noise. $l_k = 5$, $d_k = 0.7$, $l_k d_k = 3.5$, and $n_k(t) = 1$ if $t = 0.9 + 0.9(m-1)$, $m = 1, 2, 3, \dots$, and $n_k(t) = 0$ otherwise, for $k = i, j$.

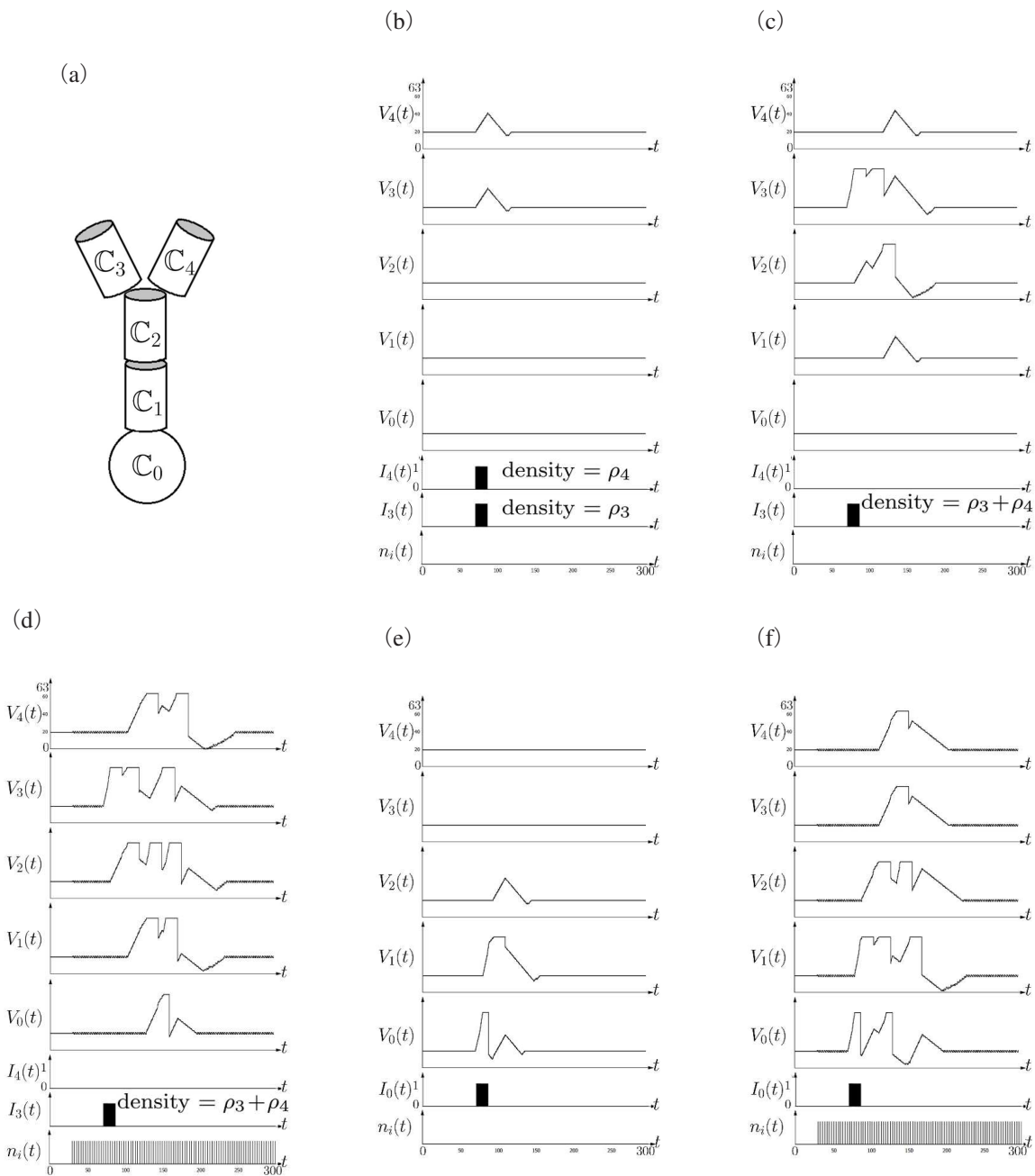
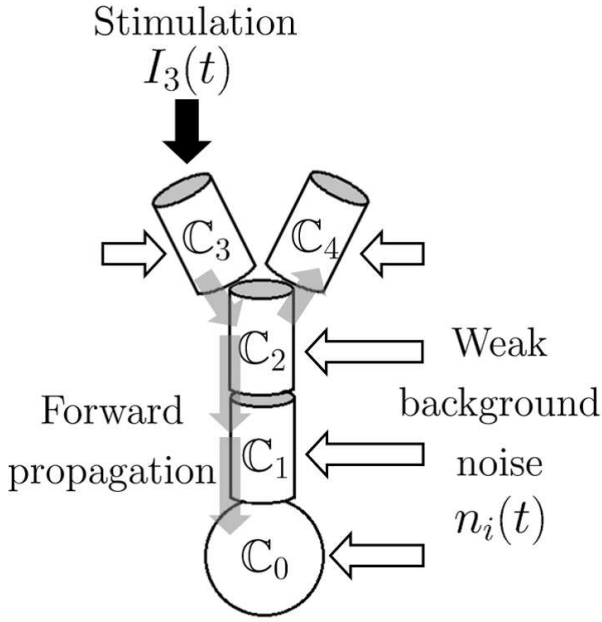


Fig. 5. (a) An example of the multi-compartment neuron model. $P = 5$, $w_{ij} = 1$ if $(i, j) = (0, 1), (1, 0), (1, 2), (2, 1), (2, 3), (2, 4), (3, 2),$ and $(4, 2)$, and $w_{ij} = 0$ if otherwise. Soma C_0 : $(M_0, N_0, f_{01}, f_{02}, f_{03}, f_{04}, f_{05}) = (64, 64, 3.5, 0.45, -0.05, 1.5, -0.43)$, $A_0(U_0) = 15$, $l_0 = 40$, $d_0 = 0.2$. Dendrites C_i , $(i = 1, \dots, 4)$: $(M_i, N_i, f_{i1}, f_{i2}, f_{i3}, f_{i4}, f_{i5}) = (64, 64, 3.5, 0.45, -0.05, 1.5, -0.43)$, $A_i(U_i) = \left\lfloor -0.9 \left(\frac{U_i - |0.1M_i|}{M} \right)^2 N_i \right\rfloor + \lfloor 0.95N_i \rfloor$, $l_i = 40$, $d_i = 0.4$. (b) Failure of forward propagation of potential. $q_m^3 = q_m^4 = 71 + 0.44(m-1)$, $71 \leq q_m^3, q_m^4 < 87$, and $(m = 1, 2, 3, \dots)$. Density $\rho_3 = \rho_4 = 1/d_3 = 1/d_4 = 2.28$. (c) Failure of forward propagation of potential. $q_m^3 = 71 + 0.22(m-1)$, $71 \leq q_m^3 < 87$, and $(m = 1, 2, 3, \dots)$. Density $\rho_3 + \rho_4 = 4.56$. (d) Forward propagation of potential. $q_m^3 = 71 + 0.22(m-1)$, $71 \leq q_m^3 < 87$, and $(m = 1, 2, 3, \dots)$. $n_i(t) = 1$ if $t = 30 + 3(m-1)$ and $(m = 1, 2, 3, \dots)$, and $n_i(t) = 0$ otherwise. Density $\rho_3 + \rho_4 = 4.56$. (e) Failure of backward-propagation of potential. $q_m^0 = 71 + 0.22(m-1)$, $71 \leq q_m^0 < 87$, and $(m = 1, 2, 3, \dots)$. (f) Backward-propagation of potential. $q_m^0 = 71 + 0.22(m-1)$, $71 \leq q_m^0 < 87$, and $(m = 1, 2, 3, \dots)$. $n_i(t) = 1$ if $t = 30 + 3(m-1)$ and $(m = 1, 2, 3, \dots)$, and $n_i(t) = 0$ otherwise for $i = 0, \dots, 4$.

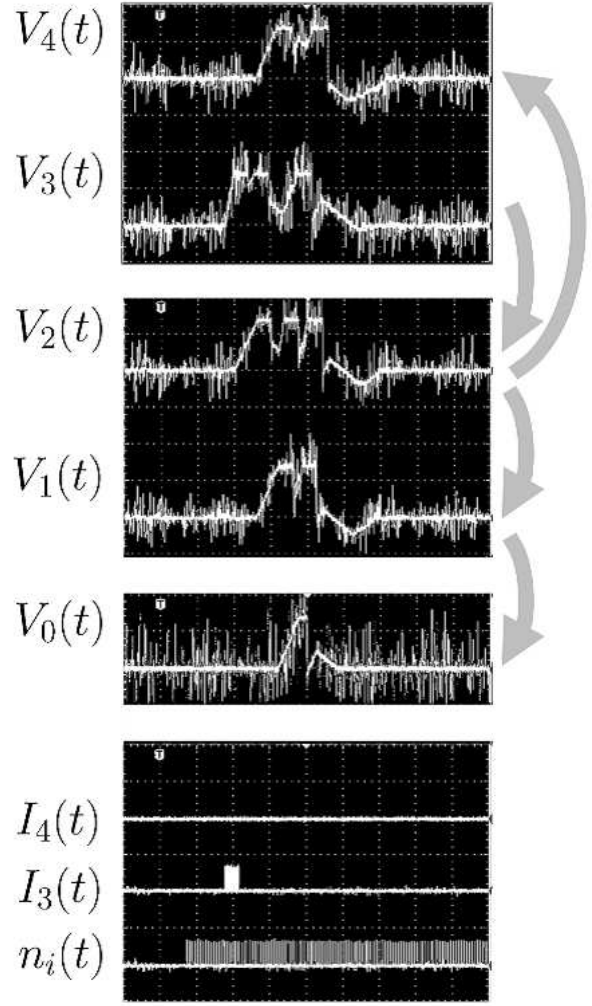
Forward propagation. If an action potential in a terminal compartment propagates to the somatic compartment C_0 directly or through relay compartments, then the propagation is referred to as a *forward propagation*.

Backward propagation. If an action potential in the somatic

compartment C_0 propagates to a terminal compartment directly or through relay compartments, then the propagation is referred to as a *backward propagation*.



(a)



(b)

Fig. 6. (a)Forward propagation. (b)Oscilloscope snapshot of the forward propagation. Horizontal axis is 4ms/div. Vertical axes are V_i : 500mV/div. and I_0 , I_3 , I_4 , and n_i : 5V/div..

Figs. 5(b) – (f) show typical numerical simulation results. In Fig. 5(b), weak external stimulation spike-trains $I_3(t)$ and $I_4(t)$ are applied to the terminal compartments C_3 and C_4 , respectively. In this case, no action potential is generated. In Fig. 5(c), a strong external stimulation spike-train $I_3(t)$ is applied to the terminal compartment C_3 , where the strength of this strong external stimulation spike-train is same as the sum of the strengths of the weak stimulation external stimulation spike-trains in Fig. 5(b). In this case, the compartment C_3 generates an action potential but it fails to propagate to the somatic compartment C_0 . So, this is a failure of forward propagation. In Fig. 5(d), the same strong external stimulation spike-train $I_3(t)$ as Fig. 5(c) is applied to the terminal compartment C_3 . In addition, a weak background spike-train $n_3(t)$ is additionally added to each compartment C_i , i.e.,

$$\begin{aligned} S_3(t) &= Z_3(t) + I_3(t) + n_3(t), \\ S_i(t) &= Z_i(t) + n_i(t) \text{ for } i \neq 3. \end{aligned}$$

In this case, the compartment C_3 generates an action potential and it propagates to the somatic compartment C_0 . So, this is a forward propagation. In Fig. 5(e), a weak external stimulation spike-train $I_0(t)$ is applied to the somatic compartment C_0 . In this case, an action potential is generated but it fails to propagate to a terminal compartment. So, this is a failure of backward propagation. In Fig. 5(f), a strong external stimulation spike-train $I_0(t)$ is applied to the somatic compartment C_0 . In addition, a weak background spike-train $n_3(t)$ is additionally added to each compartment C_i . In this case, the compartment C_0 generates an action potential and it propagates to the terminal compartments C_3 and C_4 . So, this is a backward propagation.

III. FPGA IMPLEMENTATION

The presented multi-compartment neuron model is implemented in a *field programmable gate array* (ab. FPGA). The dynamics of the model is described by Equations (1), (2),

TABLE I
COMPARISON OF HARDWARE COSTS. OCCUPIED COMPONENTS IN
XILINX'S FPGA XC7Z020-1CLG484.

	Presented model	Multi-compartment Izhikevich model
Number of slice registers	157	302
Number of slice LUTs	698	6,874
Number of occupied slices	249	1,898

(3), (4), and (5), which are written in a VHDL source code. A bitstream file for the FPGA configuration is generated by Xilinx's design software environment ISE 14.4. Parameters of the model and specifications of the resulting FPGA are summarized in Table 1, where binary coding is automatically used to represent the discrete states by the ISE. The clock $C(t)$ is generated by an on-board 100[MHz] clock and a frequency divider. Since the FPGA and the design software we used do not support for asynchronous triggering, the external stimulation spike-train $I_i(t)$ is sampled at the on-board clock frequency. Note that the sampling of $I_i(t)$ is not necessary if a target FPGA supports for asynchronous triggering. Fig. 6(b) show an oscilloscope snapshots of forward propagation, which corresponds to Fig. 5(d).

In addition, comparisons to a multi-compartment model of Izhikevich's simple neuron model [9] is summarized in Table 1. It should be emphasized that the presented model consumes less hardware resources (almost 1/7) compared to the multi-compartment model of Izhikevich's simple neuron model, where both models are fairly optimized.

IV. CONCLUSIONS

In this paper, we have presented the novel multi-compartment neuron model based on the asynchronous cellular automaton neuron model. We have shown the model can reproduce the typical propagations of action potentials observed in representative multi-compartment ODE neuron models. We have also shown the model occupies much less hardware resources than the multi-compartment Izhikevich's model. Future problems are including the following ones: (a) generalization of the presented multi-compartment model, (b) development to a synaptic compartment, and (c) reproduction of other complicated properties in dendrites.

The authors would like to thank Professor Toshimitsu Ushio of Osaka Univ. for valuable discussions. This work was partially supported by the support center for advanced telecommunications technology research (SCAT) and KAK-ENHI Grant Number 24700225.

REFERENCES

- [1] A. L. Hodgkin and A. F. Huxley, "A Quantitative Description of Membrane Current and its Application to Conduction and Excitation in Nerve," *J. Physiology*, vol. 117, no. 4, pp. 500–544, 1954.
- [2] E. M. Izhikevich, "Which Model to Use for Cortical Spiking Neurons?" *IEEE Trans. Neural Networks*, vol. 15, no. 5, pp. 1063–1070, 2004.
- [3] T. Hishiki and H. Torikai, "A Novel Rotate-and-Fire Digital Spiking Neuron and its Neuron-Like Bifurcations and Responses," *IEEE Trans. Neural Networks*, vol. 22, no. 5, pp. 752–767, 2011.

- [4] T. Matsubara, H. Torikai, and T. Hishiki, "A Generalized Rotate-and-Fire Digital Spiking Neuron Model and its On-FPGA Learning," *IEEE Trans. Circuits and Systems II*, vol. 58, no. 10, pp. 677–681, 2011.
- [5] M. Häusser and B. Mel, "Dendrites: bug or feature?" *Current Opinion in Neurobiology*, vol. 13, no. 3, pp. 372–383, 2003.
- [6] A. T. Schaefer, M. E. Larkum, B. Sakmann, and , "Coincidence detection in pyramidal neurons is tuned by their dendritic branching pattern," *J. Neurophysiology*, vol. 13, no. 3, pp. 372–383, 2003.
- [7] P. Vetter, A. Roth, and M. Häusser, "Propagation of action potentials in dendrites depends on dendritic morphology" *J. Neurobiology*, vol. 85, no. 2, pp. 926–937, 2001.
- [8] Ö. Ekeberg, P. Wallen, A. Lansner, H. Traven, L. Brodin, and S. Grillner, "A Computer Based Model for Realistic Simulations of Neural Networks. I. The Single Neuron and Synaptic Interaction." *Biological Cybernetics*, vol. 65, no. 2, pp. 81–90, 1991.
- [9] E. M. Izhikevich, *Dynamical Systems in Neuroscience: The Geometry of Excitability and Bursting*. Cambridge, MA: MIT press, 2007.
- [10] W.Rall, "Electrophysiology of a Dendritic Neuron Model," *Biophysical Journal*, vol. 2, no. 2, pp. 145–167, 1962.
- [11] X.-J.Wang, "Fast burst firing and short-term synaptic plasticity: a model of neocortical chattering neurons," *Neuroscience*, vol. 89, no. 2, pp. 347–162, 1999.
- [12] N. Shimada and H. Torikai, Multi-Compartment Asynchronous Cellular Automaton and its Application for Neuron Modeling, *Proc. NOLTA*, pp. 114-117, 2013.